

Preparation of homogeneous ZnO nanoparticles via precipitation-pyrolysis with $Zn_5(CO_3)_2(OH)_6$ as precursor

HAN Yue-xin(韩跃新), DING Ya-zhuo(丁亚卓), YIN Wan-zhong(印万忠), MA Zheng-xian(马正先)

College of Resource and Civil Engineering, Northeastern University, Shenyang 110004, China

Received 24 October 2005; accepted 20 March 2006

Abstract: ZnO nanoparticles were synthesized via precipitation-pyrolysis (P&P), where the precursor zinc hydroxide carbonate ($Zn_5(CO_3)_2(OH)_6$) was obtained and then pyrolyzed. The results of TEM indicate that pyrolysis temperature is the predominant factor for controlling mean sizes of nanoparticles, ranging from 8 nm to 80 nm. Increasing the pyrolysis temperature enhances the mean size. The results of XRD show that nanoparticles are all of crystalline zincite. The mean size observed by TEM is in agreement with that calculated from the specific surface area(SSA) and the crystalline size calculated from the XRD patterns, indicating that the primary particles are rather uniform in size and have single crystals. The growth behaviors of epitaxy along the *C*-axis are responsible for the morphology of ZnO changing from sphere to rod-like shape, and then to reticulation. Compared with other synthesis approaches, P&P can get fairly good product with a relatively low cost.

Key words: ZnO; nanoparticles; precipitation-pyrolysis; precursor; morphology

1 Introduction

Recently, demands for high product performance products have necessitated a precise control of ZnO particle properties for applications such as electrode of solar cells and photocatalysts. Much attention is given to the high chemical reactivity of ZnO by increasing reactive sites and the complex nature of the UV and visible fluorescence. Therefore, a lot of efforts have been taken to precisely control particle properties of ZnO by various sophisticated manufacturing processes[1].

ZHANG et al[2] synthesized ZnO nanoparticles by precipitation mechanochemical method. But the milling process can only make part of the precursor transform into ZnO. To get pure product, the pyrolysis process is needed. ZHANG et al[3] also synthesized ZnO nanoparticles with 3–5 nm in diameter by sol-gel. STASSINOPoulos et al[4] investigated the surface modification of ZnO film. Surface processing employing laser annealing transforms the particulate grain structure of the as-deposited films into a porous channel-like network, which is shown to be critical for achieving

random laser action as it favors efficient coupling of the pump light into the film material. LIU et al[5] prepared a kind of novel bulk ZnO porous nanosolids by a unique solvothermal hot-press method, using ZnO nanoparticles and several kinds of solvents as the starting materials. And “self-assembly process” of ZnO nanoparticles was found. WANG et al[6] controlled the growth of ZnO by adding H_2O , during which wurtzite ZnO particles were synthesized via $Zn(CH_3COO)_2$ hydrolyzing in methanol using chemical deposition method. JI et al[7] synthesized ZnO nano-film by three-step-method (oxidizing metallic Zn by H_2O_2 , spraying to make substrate and annealing).

But the processes above have many difficulties in mass production. So it is necessary to look for an industrial process which can synthesize homogeneous ZnO nanoparticles cheaply.

FSP (flame spray pyrolysis) is a popular method in Europe and Japan[1, 8–12], by which the particle size can be controlled in 10–20 nm with feed rate of 1–4 mL/min, and the cost can be controlled below 5 \$/kg. FEAG (filter expansion aerosol generator) method[13–16] is also good in synthesizing nanoparticles and ZnO particles of 12 nm was obtained.

In this study, the synthesis of crystalline ZnO nanoparticles with closely controlled size and morphology by P&P (precipitation-pyrolysis) are investigated. The effects of reaction time/temperature, original concentration of Zn^{2+} , pyrolysis time/temperature and the ratio of Zn^{2+} to CO_3^{2-} on the ZnO particle sizes are reported. The pyrolysis and crystal process are investigated. And a comparison on particle sizes is made between P&P and other processes.

2 Experimental

$ZnCl_2$ and Na_2CO_3 (AR) were used as starting materials. The flow sheet is shown in Fig.1.

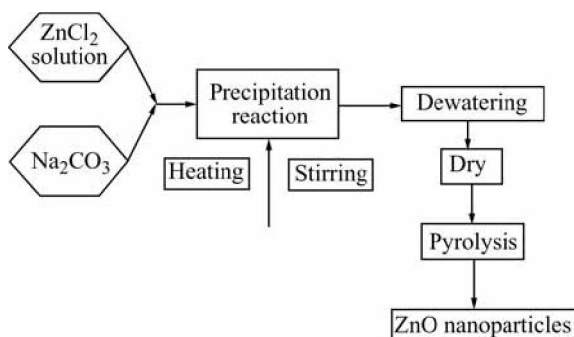


Fig.1 Flow sheet of synthesis of ZnO nanoparticles via P&P

The specific surface area(SSA) of the particles was measured by 5-point nitrogen adsorption (BET: Beijing ST-08) after degassing the powder at 150 °C for 2 h in nitrogen. The d_{BET} was calculated from the measured SSA and the density of ZnO ($\rho_{ZnO}=5.61 \times 10^3 \text{ kg/m}^3$): $d_{BET}=6/(A_{SSA} \cdot \rho_{ZnO})$. The powder crystallinity was measured by XRD (Rigaku, D/max-rA, 40 kV, 50 mA) at 2θ ($Cu K\alpha$)=20°–70° with the step of 0.02° and scan speed of 0.24(°)/min. The d_{XRD} was calculated from the full width at half maximum (FWHM) of the (100) peak using Scherrer's equation (Klug & Alexander, 1974): $d_{XRD}=0.9 \times \lambda/(\beta-\beta')\cos\theta$, where λ is a wavelength of the X-ray (0.154 05 nm) and β , β' and θ represent the measured FWHM, the broadening of a peak caused by the equipment and a diffraction angle, respectively. The β' was determined by measuring the FWHM of the (100) peak using the ZnO particles of several microns in diameter. The particle morphology was observed by TEM (Philips EM400T). The general thermal analysis was carried out (America, STD600).

3 Results and discussion

Fig.2 shows the precursor's XRD pattern and $Zn_5(CO_3)_2(OH)_6$ is found.

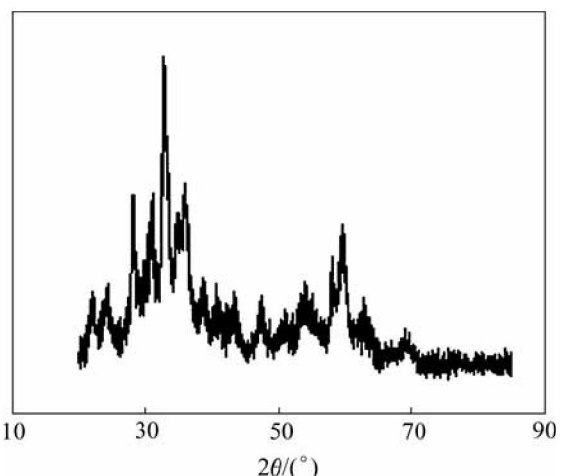


Fig.2 X-ray diffraction pattern of precursor $Zn_5(CO_3)_2(OH)_6$

Fig.3 shows the effects of reaction temperature and time, original concentration of Zn^{2+} , ratio of CO_3^{2-} to Zn^{2+} , pyrolysis temperature and time on ZnO particle properties.

From Fig.3, it is shown that the predominant factor to control particle size is pyrolysis temperature (8–80 nm), and pyrolysis also has an influence on particle size; while other conditions have less influence on the properties of ZnO nanoparticles. The optimized experiment was carried out on the pyrolysis temperature and time.

From Table 1 and Fig.4, when pyrolysis temperature is 300 °C, the pyrolysis time has little influence on particle size. While pyrolysis temperature reaches 400 °C and 500 °C, the pyrolysis time has great influence on it.

Table 1 Results of optimized experiment (particles size/nm) on pyrolysis temperature and time

Pyrolysis temperature/ °C	Pyrolysis time/h			
	1	2	3	4
300	9.5	13.8	16.8	22.8
400	10.9	18.7	70.6	71.3
500	20.8	50.7	90.6	110.5

Fig.5 shows the TEM images of ZnO nanoparticles under different pyrolysis temperatures and time.

We also find that the morphology of the ZnO nanoparticles changes with the increase of pyrolysis temperature.

From Fig.6 we can see that the morphology of P&P-made ZnO particles changes from sphere or sphere-like shape to short rod then net-structure with the increase of temperature. This result can be explained by

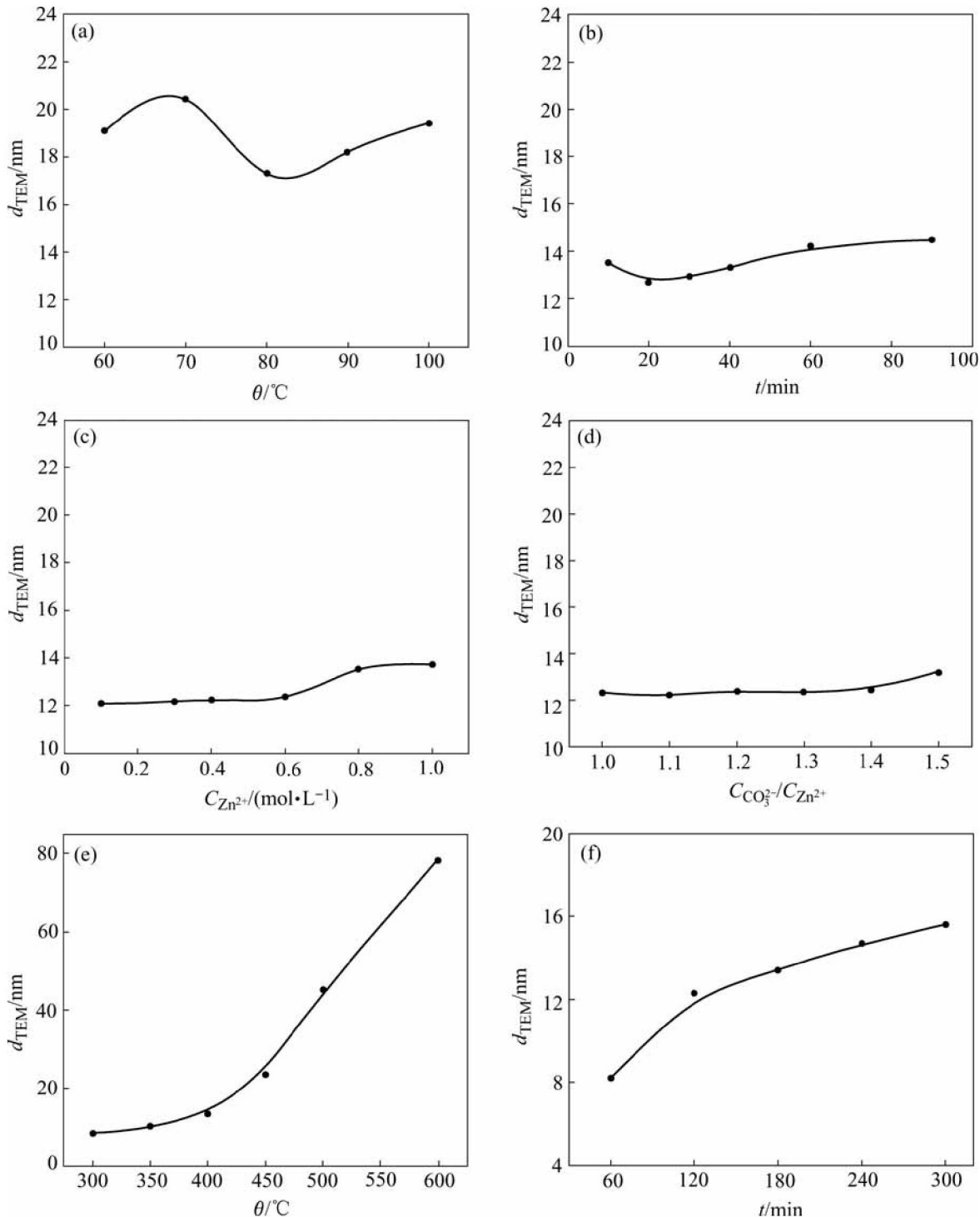


Fig.3 Effects of different conditions on nano-ZnO particle size: (a) Reaction temperature; (b) Reaction time; (c) Original concentration of Zn^{2+} ; (d) Ratio of $C_{\text{CO}_3^{2-}}/C_{\text{Zn}^{2+}}$; (e) Pyrolysis temperature; (f) Pyrolysis time

the crystal growth behaviour of ZnO nanoparticles under the condition of high temperature. As molecule of ZnO is polar, the intergrowth behaviour along C axis as shown in Fig.7 is found because of static effect [17]. From energetic point of view, with the increase of the temperature, the C -axis interfaces of nanoparticles tend to be more active and interattracted. There is an

agreement between the observed results in Fig.6 and those of ZnO nano-particles synthesized by P&P using $\text{ZnC}_2\text{O}_4\cdot 2\text{H}_2\text{O}$ as precursor[18]. The growth procedure can be illustrated in Fig.8. First, the connection of the particles is realized by the static effect, but the force is low, and they can be scattered by surface modifying or ultrasonic device (Fig.9). But with the increase of the

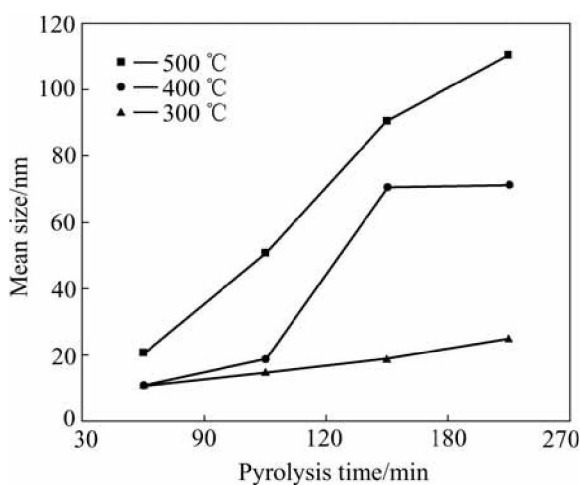


Fig.4 Results of optimized experiment on pyrolysis temperature and time

temperature, the surfaces of *C*-axis connect firmly, the interfaces disappear, and rod-like particles and reticulum are formed.

Fig.10 shows the result of TG-DTA-DTG test for the precursor. The initial temperature of loss mass is about 200 °C, with the ending temperature of 280 °C. The mass loss of 26% is in good agreement with theore-

tic value (25.9%), indicating that the pyrolysis reaction follows Eqn.(1):



It has been confirmed that the process of $\text{Zn}_5(\text{CO}_3)_2(\text{OH})_6$ pyrolysis is a solid phase reaction, through which the mechanism model of pyrolysis process, Random Nucleation Aurami II Equation was reported in another paper[19].

Fig.11 shows the XRD patterns of the as-prepared powders under different pyrolysis temperatures. All powders are hexagonal zincite (#36-1451) and no secondary or amorphous phase is observed. The height of peaks increases and the width of peaks decreases as the pyrolysis temperature increases, which indicates the crystallite growth.

Fig.12 shows that X-ray diffraction crystalline size calculated using Scherrer's equation and BET equivalent average primary particle diameter (d_{BET} : triangles) are in good agreement with each other as well as apparent sizes observed by TEM for the powders below 50 nm, indicating low degree of agglomeration (necking) and single crystals. This result is in agreement with the experience that "the measurement values are close to the real values as the crystalline size is below 50 nm"[20].

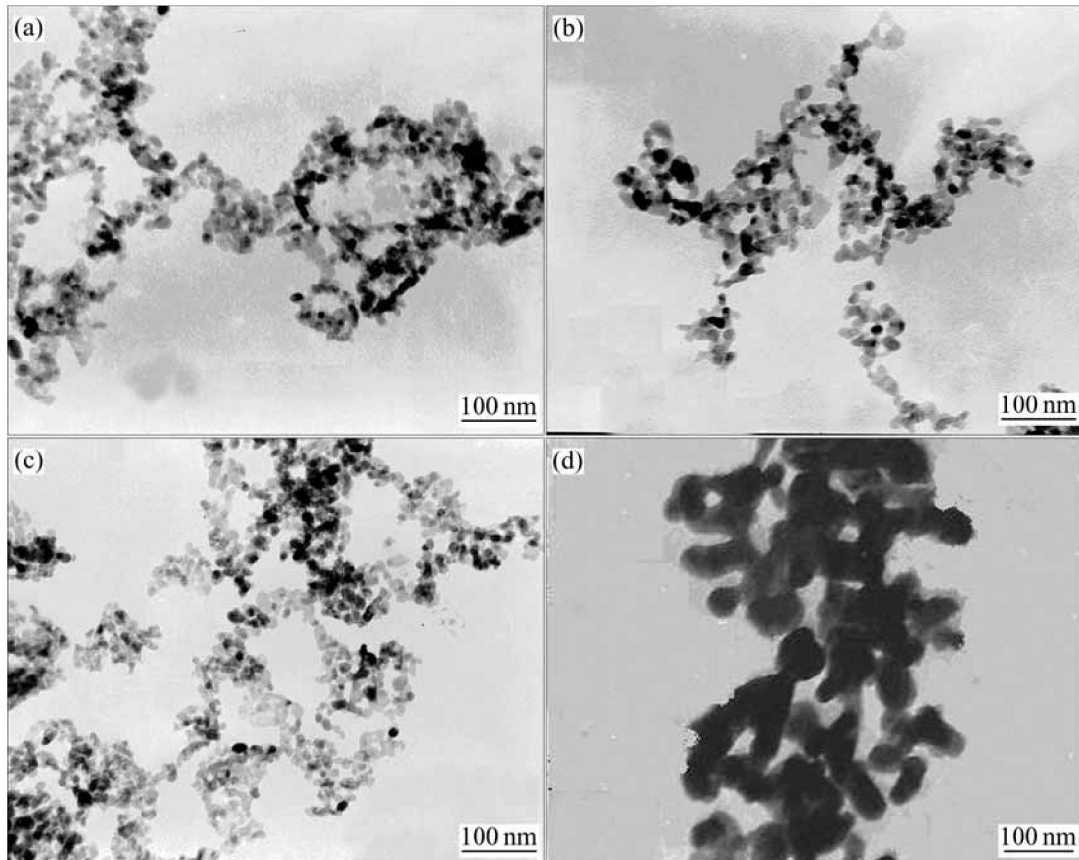


Fig.5 TEM images of ZnO nanoparticles under different pyrolysis temperatures and times: (a) 300 °C, 60 min; (b) 300 °C, 240 min; (c) 400 °C, 60 min; (d) 400 °C, 240 min

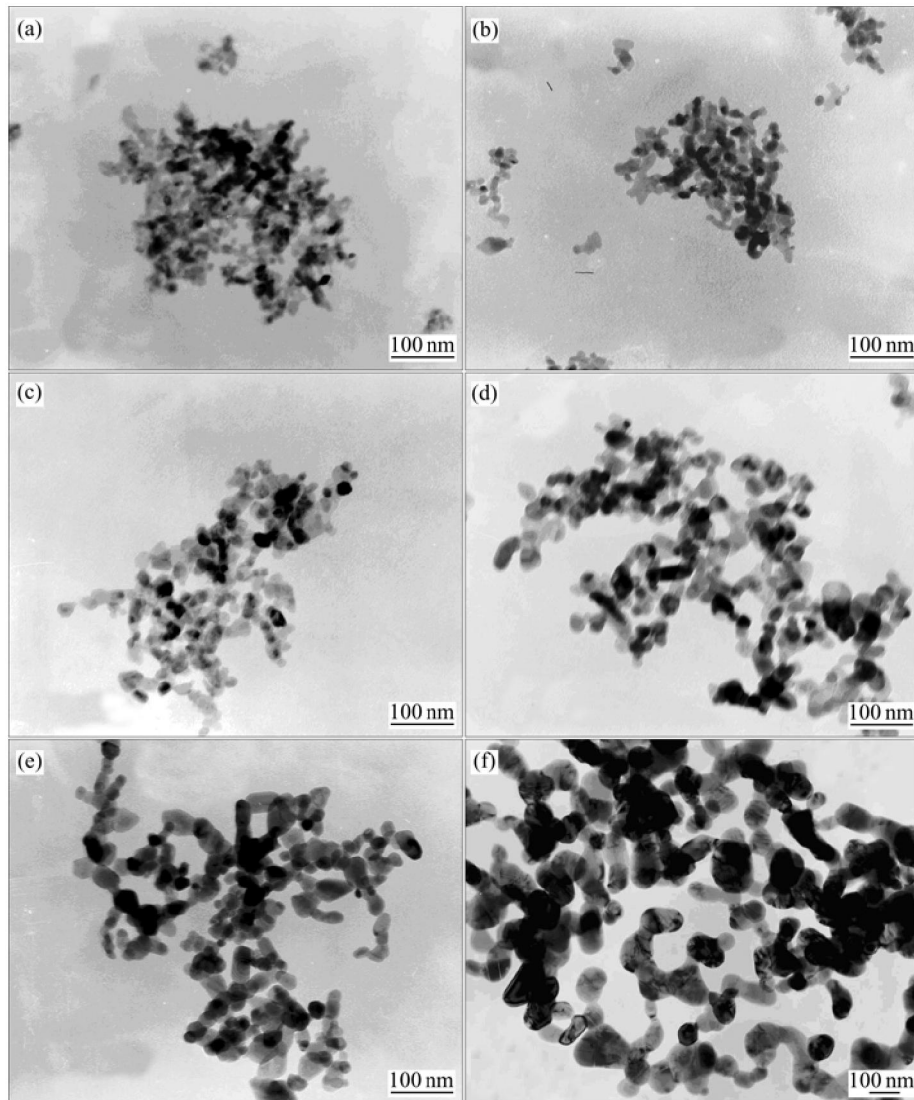


Fig.6 TEM images of P&P-made ZnO particles under different pyrolysis temperatures: (a) 300 °C; (b) 350 °C; (c) 400 °C; (d) 450 °C; (e) 500 °C; (f) 600 °C

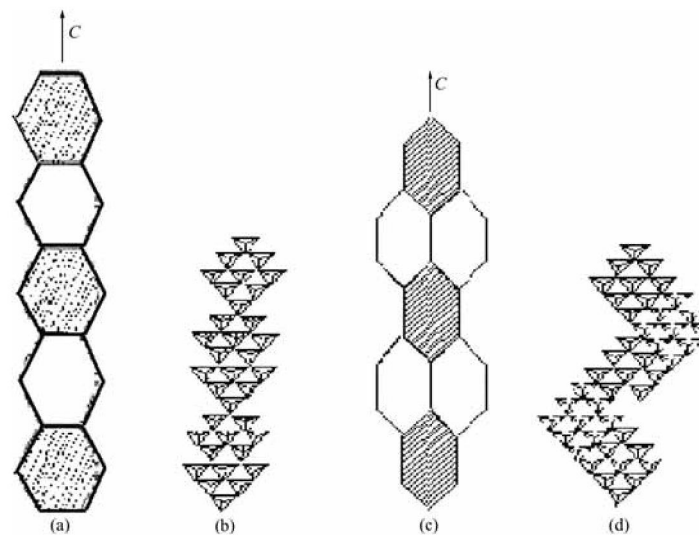


Fig.7 Epitaxy behaviour of ZnO nanoparticles[17]: (a) Intergrowth on positive and negative polar faces; (b) $[ZnO_4]^{6-}$ tetrahedrons connection on positive and negative polar faces; (c) Intergrowth on positive and negative cone faces; (d) Accordant connection of $[ZnO_4]^{6-}$ tetrahedrons on positive and negative cone faces

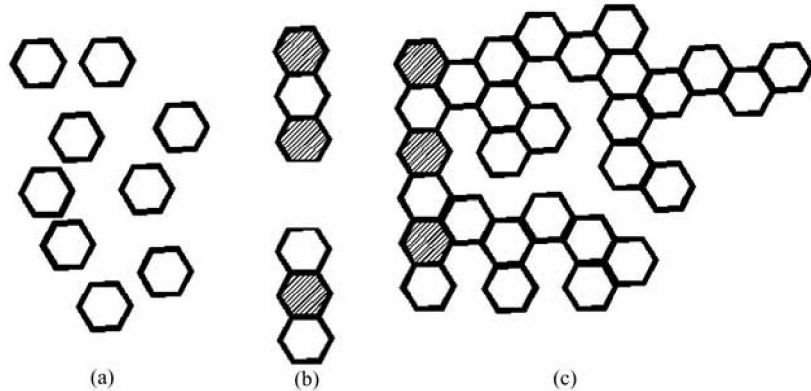


Fig.8 Growth procedure of ZnO nanoparticles: (a) Particles structure; (b) Rod-like structure; (c) Reticulum

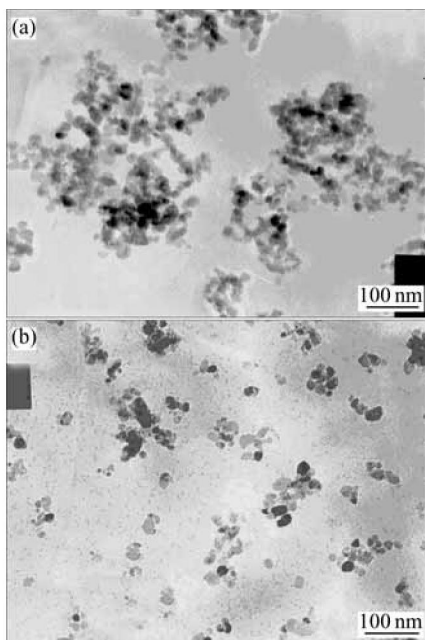


Fig.9 TEM images before modification(a) and after modification(b) of nano-ZnO by coupling agent (Synthetic condition: pyrolysis time 2 h, pyrolysis temperature 350°C, modification agent titanic acid ester coupling agent)

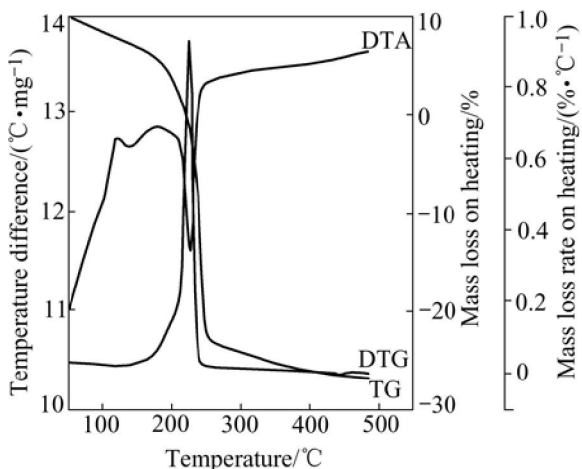


Fig.10 Thermal analysis for precursor

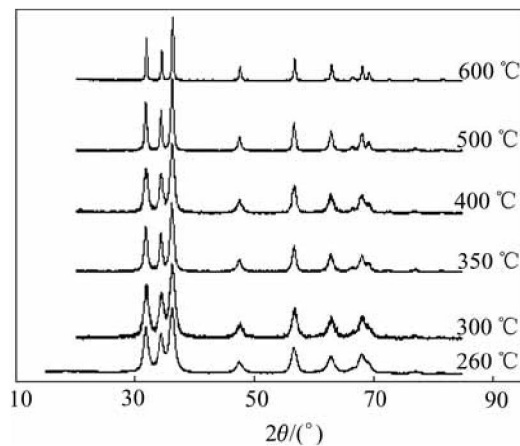


Fig.11 XRD patterns of ZnO nanoparticles under different pyrolysis temperatures

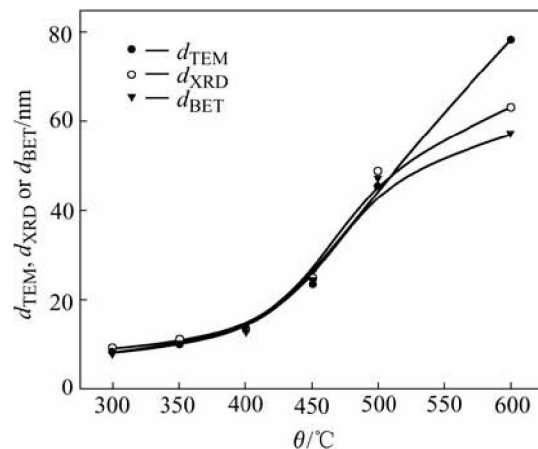


Fig.12 Comparsion of d_{XRD} , d_{TEM} and d_{BET} under different pyrolysis temperatures (synthetic condition: reaction temperature 60°C, reaction time 30 min, original concentration of Zn^{2+} 0.5 mol/L, ratio of $C_{CO_3^{2-}}$ to $C_{Zn^{2+}}$ 1.1, pyrolysis time 2 h)

Fig.13 shows that ZnO nanoparticles synthesized by P&P show good performance on particle size compared with particles by other processes. FSP and FEAG can synthesize ZnO nanoparticles about 10 nm. Smaller particles can be obtained by sol-gel, but the cost and

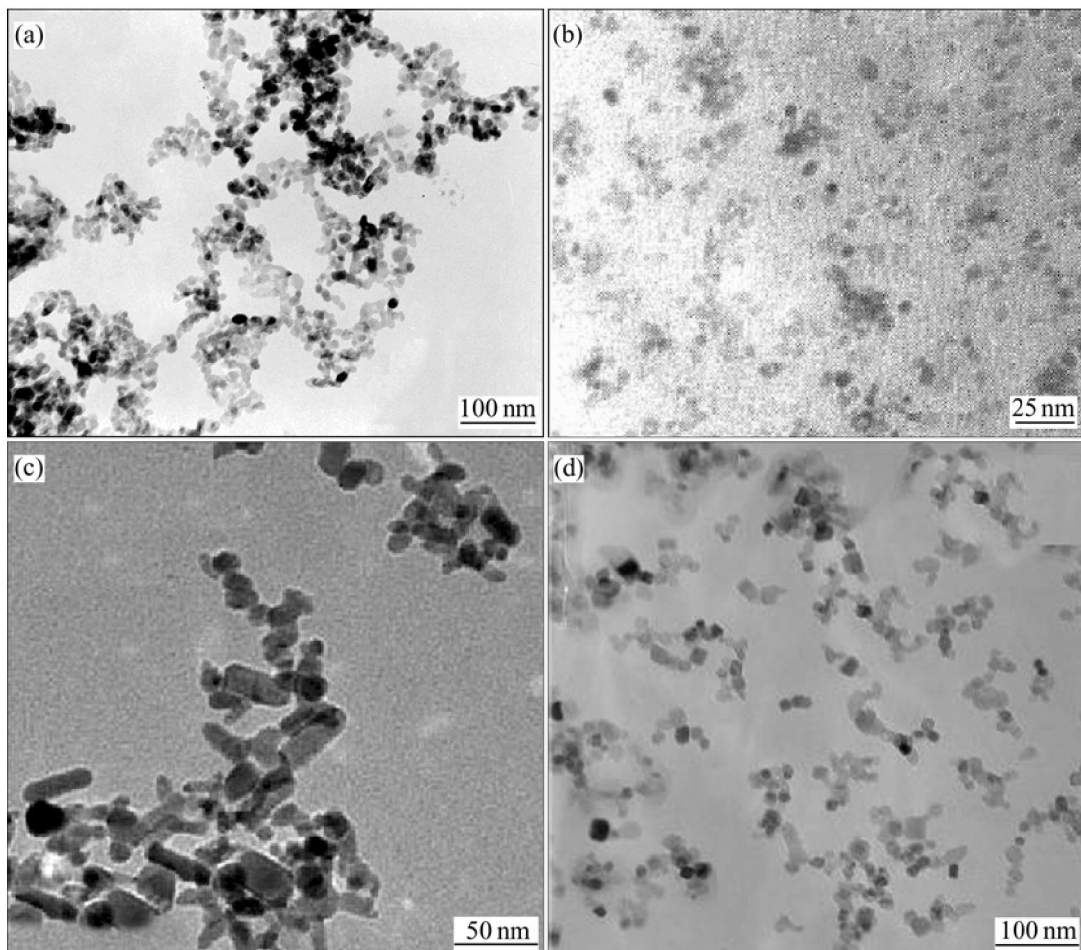


Fig.13 TEM morphologies of ZnO nanoparticles by different methods: (a) P&P (pyrolysis time 2 h, pyrolysis temperature 300 °C); (b) Sol-gel[2] (time of aging 4 h); (c) FSP[1] (solution feed rate 3 mL/min); (d) FEAG[16] (reactor temperature 800°C)

complex procedures limit its application. And P&P is a competitive method in mass production.

4 Conclusions

1) Crystalline ZnO nanoparticles of less than 10 nm in primary particle diameter are produced by P&P. The primary particle diameter increases from 8 to 80 nm as the pyrolysis temperature increases from 300 to 600 °C. The growth behaviour of C-axis changes the ZnO's morphology from sphere to short rod and then reticulation.

2) The primary particles are uniform in diameter and have single crystals. Compared with the ZnO nanoparticles by other methods, the P&P-made powder is one of the smallest and most homogeneous ones, and P&P is suitable to produce ZnO nanoparticles industrially.

References

[1] TANI T, LUTZ M, PRASITINIS S E. Homogeneous ZnO

nanoparticles by flame spray pyrolysis [J]. *Journal of Nanoparticles Research*, 2002, 4(4): 337–343.

- [2] ZHANG Shi-cheng, LI Chun-he, LI Xing-guo. Size control and characterization of ZnO nanoparticles [J]. *Acta Phys-Chim Sin*, 2004, 20(special): 902–905.
- [3] ZHANG S C, CHI L, LI X G. Preparation of ZnO nanoparticles by precipitation/mechanical method [A]. SHIMOMURA M, ISHIHARA T. *Proceedings of Asianano 2002* [C]. World Scientific PUBL Co PTE Ltd, Singapore: 2003, 189–193.
- [4] STASSINOPoulos A, DAS R N, GIANNELIS E P, ANASTASIADIS S H, ANGLOS D. Random lasing from surface modified films of zinc oxide nanoparticles [J]. *Applied Surface Science*, 2005, 247(1–4): 18–24.
- [5] LIU X L, XU H Y, YU L L, LI M, WANG C J, CUI D L, JIANG M H. Self-assembly of ZnO nanoparticles and preparation of bulk ZnO porous nanosolids [J]. *Chinese Science Bulletin*, 2005, 50(7): 612–617.
- [6] WANG H H, XIE C S, ZENG D W. Controlled growth of ZnO by adding H₂O. [J] *Journal of Crystal Growth*, 2005, 277(1–4): 372–377.
- [7] JI Z G, ZHAO S C, WANG C, LIU K. ZnO nanoparticle films prepared by oxidation of metallic zinc in H₂O₂ solution and subsequent process [J]. *Materials Science and Engineering B—Solid State Materials for Advanced Technology*, 2005, 117(1): 63–66.
- [8] MÄDLER L, KAMMLER H K, MUELLER R, PRATSINIS S E. Controlled synthesis of nanostructured particles by flame spray pyrolysis [J]. *Journal of Aerosol Science*, 2002, 33: 369–389.
- [9] TANI T, MÄDLER L, PRATSINIS S E. Synthesis of zinc oxide/silica composite nanoparticles by flame spray pyrolysis [J].

Journal of Material Science, 2002, 37: 4627–4632.

[10] PANATARANI C, WULED L, KIKUO O. Synthesis of single crystalline ZnO nanoparticles by salt assisted spray pyrolysis [J]. Journal of Nanoparticle Research, 2003, 5(1/2): 47–53.

[11] TANI T, WATANABE N, TAKATORI K. Emulsion combustion and flame spray synthesis of zinc oxide/silica particles [J]. Journal of Nanoparticle Research, 2003, 5(1/2): 39–46.

[12] JENSEN J R, JOHANNESSEN T, WEDEL S, LIVBJERN H. Preparation of ZnO/Al₂O₃ particles in a premixed flame [J]. Journal of Nanoparticles Research, 2000, 2(4): 363–373.

[13] YUN C K, PARK S B. A high-volume spray aerosol generator producing small droplets for low pressure applications [J]. Journal of Aerosol Science, 1995, 26(7): 1131–1138.

[14] PARK S B, YUN C K. Photocatalytic activity of nanometer size ZnO particles prepared by spray pyrolysis [J]. Journal of Aerosol Science, 1997, 28(Supplement 1): S473–S474.

[15] KANG Y C, CHOI J S, PARK S B, CHO S H, YOO J S, LEE J D. Preparation of CaTiO₃:Pr phosphor by spray pyrolysis using filter expansion aerosol generator [J]. Journal of Aerosol Science, 1997, 28(Supplement 1): S541–S542.

[16] KANG Y C, PARK S B. Preparation of zinc oxide-dispersed silver particles by spray pyrolysis of colloidal solution [J]. Materials Letters, 1999, 40: 129–133.

[17] LIU Chao-feng, ZHENG Yan-qing, ZHONG Wei-zhuo, WANG Zhen-hong, HU Xing-fang. Epitaxy of ZnO nanocrystal [J]. Journal of Synthetic Crystals, 1999, 28(8): 244–248.

[18] YIN Wan-zhong, DING Ya-zhuo, HAN Yue-xin, YUAN Zhi-tao. Preparation of ZnO nanoparticles using zinc oxalate dihydrate as the precursor [J]. Journal of Northeastern University (Nature Science), 2005, 6(6): 585–587.

[19] MA Zheng-xian, HAN Yue-xin, LIU Chun-shen, ZHENG Long-xi, WANG Ze-hong. Study on mechanism and kinetics of thermal decomposition of zinc hydroxide carbonate [J]. Engineering Science, 2003, 5(10): 78–82.

[20] ZHANG Li-de, MOU Ji-mei. Nano Materials and Nano Structures [M]. Beijing: Science Express, 2001.

(Edited by YANG Bing)